Light Localization Characteristics in a Random Configuration of Dielectric Cylindrical Columns

Yuta Inose,[1,2] Masaru Sakai,[3] Kazuhiro Ema,[1,2,4] Akihiko Kikuchi,[1,2,4] Katsumi Kishino,[1,2,4] and Tomi Ohtsuki[1,2,4]

[1]*Sophia University, 7-1 Kioi-cho, Chiyoda-ku, Tokyo 102-8554, Japan*
[2]*CREST, Japan Science and Technology Agency, Japan*
[3]*University of Yamanashi, 4-3-11 Takeda, Kofu, Yamanashi 400-8511, Japan*
[4]*Sophia Nanotechnology Research Center, Sophia University, Japan*

(Dated: October 28, 2010)

In the two-dimensional random system composed of a disordered array of dielectric cylindrical columns, Anderson localization of light occurs. To obtain frequency dependence of the light localization characteristics, we have simulated temporal diffusion of electromagnetic waves in such a random system adopting parameters of actual nano-sized semiconductor samples with a high filling fraction of the columns, using the finite-difference time-domain method. We have investigated diffusion length, autocorrelation function of light energy density, and time variation of total energy within the system at several frequencies. We obtain universal behavior of light localization phenomenon as a function of the light localization length and system size, from which we estimate frequency dependence of the localization length. In addition, we show that the frequency dependence of the localization effect depends on the degree of wave interference due to Bragg-like diffraction, rather than on the magnitude of the light scattering cross section of a single scatterer.

PACS numbers: 42.25.Dd, 42.55.Zz, 02.70.Bf, 78.67.Qa
Keywords: Anderson localization, light localization, random laser, localization length, diffusion length, autocorrelation function, finite-difference time-domain, FDTD, nanocolumn, nanorod, photonic crystal

I. INTRODUCTION

The possibility of Anderson localization of light in a random dielectric system, namely spatial electromagnetic wave localization similar to electron wave localization in a disordered solid, has been studied extensively over the last three decades.[1–3] It is predicted that the light localization effect in random media has strong frequency dependence. To realize strong localization, the photon mean free path l must be nearly equal to the wavelength of light λ.[3,4] However, it is not easy to derive the specific parameters for strong localization. For example, theoretical approaches for the effect are rather limited because the light propagation problem on the random system is analytically insoluble. In addition, the localization effect is hard to observe experimentally because of the various randomness of actual samples, and observations of light localization have been realized only recently.[5,6]

A promising experimental approach for random semiconductor samples is to observe random lasing, which appears as a result of light localization. Random lasing is expected to occur if optimal parameters for obtaining strong light localization effects are met at a wavelength that lies within the emission range of the semiconductor. This phenomenon is realized because the localization effect by the random media plays the role of an optical resonator; and the random media also serve as gain media at the emission wavelength. Random lasing using randomly arrayed nano-sized semiconductors has been observed for zinc oxide (ZnO) powders[7–9] in a three-dimensional (3D) system, and on ZnO nanocolumns[10,11] in a two-dimensional (2D) system. Besides ZnO, random lasing also has been observed on gallium nitride (GaN) nanocolumns,[12] which form a 2D system. In a 3D random system, it is difficult to achieve the required uniformity of scatterer size and observe spatial distributions of the localization effect inside the samples. On the other hand, in a 2D system such as semiconductor nanocolumns, it is much easier to confirm the uniformity and observe localization states experimentally.

In this paper, we have simulated light propagation in GaN nanocolumns[13] via the finite-difference time-domain (FDTD) method.[14] The simulated sample consisted of parallel nano-sized columnar semiconductor crystals. The diameter of the nanocolumns was varied from about 50 to 400 nm, column heights were around 1 μm, and the filling fraction of the columns was approximately 0.4. For the purpose of inspecting frequency dependence of the light localization, we describe the frequency dependencies of diffusion length, autocorrelation function and photon lifetime with a fixed column diameter and a fixed filling fraction, and discuss the light localization characteristics using these quantities.

The paper is organized as follows. In Sec. II, we explain the numerical calculation method. In Secs. III and IV, we show results for energy diffusion length and energy autocorrelation function, and discuss the regime where the localization length is smaller than the system size. In Sec. V, we show photon lifetime of the system and discuss the frequency dependence of the localization effect in detail. We discuss the scaling behavior of the quality factor as a function of the ratio between the localization length and system size, from which we show frequency dependence of the localization length in Sec. VI. Lastly, we consider the physical origin of the light localization in Sec. VII.

II. NUMERICAL CALCULATION METHOD

In the infinite-size 2D disordered system, all states of a light wave are expected to be localized.[15] On the other hand, in the finite-size random system, those states for which the localization length ξ is smaller than the system size L_{sys} are regarded

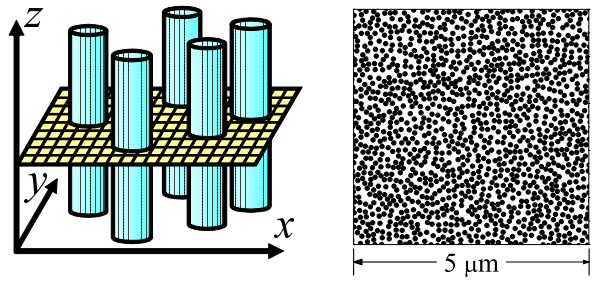

(a) Schematic view of the 2D FDTD model.

(b) Top view of column configuration of a 5 μm square.

FIG. 1. (Color online) Schematic view and top view of the 2D FDTD system for a cylindrical column ensemble. In our simulation, the height of the columns is set to be infinity.

as the *localized states*, while the states with ξ larger than $L_{\rm sys}$ are regarded as the *effectively delocalized states* where light waves diffuse rapidly. To observe the localization effect in the finite-sized system composed of the columns, the radius of the columns R, the column filling fraction Φ, the refractive index of the columns n, and the frequency of electromagnetic waves f must be properly tuned. For the purpose of studying frequency dependence of the light localization in the finite 2D system, we have simulated light propagation in a dielectric cylindrical column ensemble, by adopting the parameters of GaN nanocolumn samples.

We have used the 2D FDTD method to simulate temporal propagation of electromagnetic waves in the random medium. The FDTD method is a versatile numerical calculation method, in which Maxwell's equations are discretized using central difference approximations of the space and time partial derivatives. A schematic view of the 2D FDTD model is illustrated in Figure 1(a), where the electromagnetic waves propagate in the x-y plane. In the 2D systems, two polarizations, namely TM-polarization (electric fields E parallel to the z axis) and TE-polarization (magnetic fields H parallel to the z axis) are possible. Maxwell's equations for the TM field can be written as

$$\varepsilon_{\rm r}(\boldsymbol{r})\varepsilon_0\frac{\partial}{\partial t}E_z(\boldsymbol{r},t) = \frac{\partial}{\partial x}H_y(\boldsymbol{r},t) - \frac{\partial}{\partial y}H_x(\boldsymbol{r},t), \tag{1a}$$

$$\mu_0\frac{\partial}{\partial t}H_x(\boldsymbol{r},t) = -\frac{\partial}{\partial y}E_z(\boldsymbol{r},t), \tag{1b}$$

$$\mu_0\frac{\partial}{\partial t}H_y(\boldsymbol{r},t) = \frac{\partial}{\partial x}E_z(\boldsymbol{r},t), \tag{1c}$$

and those for the TE field as

$$\mu_0\frac{\partial}{\partial t}H_z(\boldsymbol{r},t) = -\frac{\partial}{\partial x}E_y(\boldsymbol{r},t) + \frac{\partial}{\partial y}E_x(\boldsymbol{r},t), \tag{2a}$$

$$\varepsilon_{\rm r}(\boldsymbol{r})\varepsilon_0\frac{\partial}{\partial t}E_x(\boldsymbol{r},t) = \frac{\partial}{\partial y}H_z(\boldsymbol{r},t), \tag{2b}$$

$$\varepsilon_{\rm r}(\boldsymbol{r})\varepsilon_0\frac{\partial}{\partial t}E_y(\boldsymbol{r},t) = -\frac{\partial}{\partial x}H_z(\boldsymbol{r},t), \tag{2c}$$

where ε_0 and μ_0 are the electric permittivity and magnetic permeability of vacuum, respectively. Here $\boldsymbol{r}$ denotes the position (x, y), and $\varepsilon_{\rm r}(\boldsymbol{r})$ is the relative electric permittivity. We here ignore frequency dispersion and the imaginary part of the electric permittivity, and the refractive index $n(\boldsymbol{r})$ is related to $\varepsilon_{\rm r}(\boldsymbol{r})$ by $\varepsilon_{\rm r}(\boldsymbol{r}) = n^2(\boldsymbol{r})$. The space mesh Δr is set to 5 nm, which is small enough compared with the column radius ($R = 50$ nm) and the average distance of each column a (also of the order of R). To model an open system, we used Berenger's perfectly matched layer[16] for the boundary condition in the FDTD simulation.

The sample area consists of a random array of parallel dielectric columns with a constant radius ($R = 50$ nm) and a constant refractive index ($n = 2.4$, the value for GaN at a wavelength of 500 nm). The dielectric cylindrical columns (namely circular disks in the 2D systems) are placed randomly without touching each other, and are embedded in a vacuum. Figure 1(b) shows an example of the column configuration over a 5 square μm area. Each disk represents a dielectric cylindrical column. The randomness is introduced through the positions of the columns. The column filling fraction Φ is 0.4. Unless explicitly stated, we use a system 20 μm × 20 μm in size.

For investigating frequency dependence of light diffusion characteristics, we prepared a Gaussian E_z pulse for the TM polarization and an H_z pulse for TE polarization, in the center of the simulation system, in order to generate concentric light diffusion from the point source. In the next three sections, we calculate energy diffusion length, energy autocorrelation function, and photon lifetime to study the frequency dependence of the light localization phenomenon and discuss both the localized and the effectively delocalized regimes.

III. DIFFUSION LENGTH

In this section, we have used the diffusion length $L(t)$ defined by

$$L^2(t) = \int d\boldsymbol{r}\, u(\boldsymbol{r},t)|\boldsymbol{r}-\boldsymbol{r}_0|^2, \tag{3}$$

in analogy with a random electron system,[17] where $\boldsymbol{r}_0$ is the position of the point source, t the elapsed time measured from the end of the incident pulse, and $u(\boldsymbol{r},t)$ the normalized energy density with respect to the total supplied energy at a given t. In the effectively delocalized regime of d dimensions, $L^2(t)$ is given by

$$L^2(t) \sim 2dDt \tag{4}$$

where D is the diffusion coefficient. On the other hand, in the localized regime, growth of $L^2(t)$ is suppressed and in the limit of large t is saturated at a value given by[18]

$$L^2(t) \sim \frac{d(d+1)}{4}\xi^2. \tag{5}$$

The frequency width of the incident pulse Δf is 0.05 PHz (petahertz, 10^{15} Hz), resulting in a pulse width of about

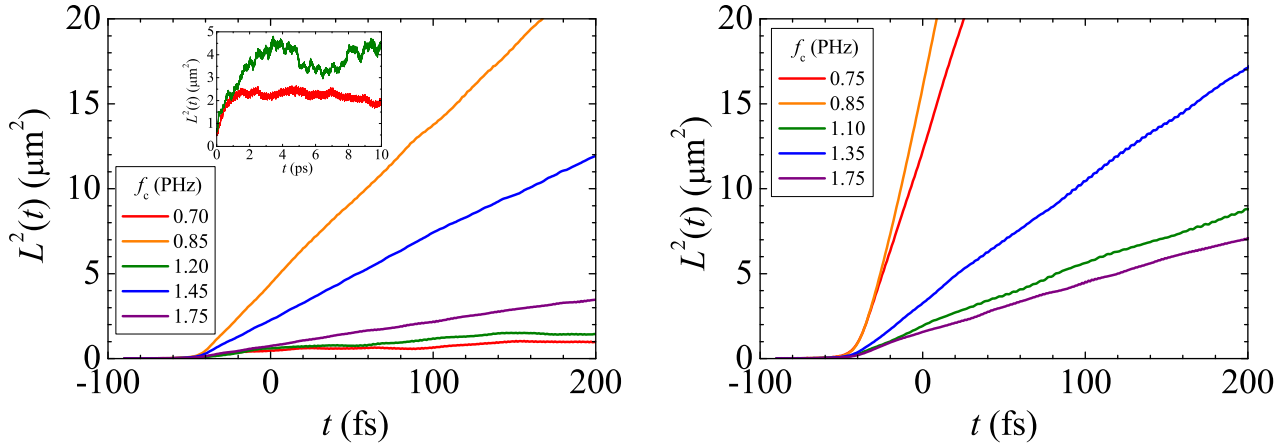

(a) TM polarization

(b) TE polarization

FIG. 2. (Color online) Diffusion length $L(t)$ for both polarizations for various f_c. The inset of (a) displays $L(t)$ at $f_c = f_1$ and f_2.

8.83 fs. The full duration of the incident pulse t_{inc}, namely the time from the front edge of the pulse to the end, is set to be 91 fs. The amplitude of the incident field at the edges of the pulse is sixteen orders of magnitude less than the amplitude at the peak. We have calculated $L(t)$ at several center frequencies of the incident pulse f_c, which ranged from 0.05 to 2.10 PHz in increments of 0.05 PHz. For the calculation of the diffusion length, no light energy must escape from the system before the incident pulse is fully injected. Therefore the above parameter of the incident pulse is selected so that the total incident energy remains inside of the sample area at $t = 0$ when the incident pulse is terminated. Note that we should use a narrow frequency width Δf for precisely investigating the frequency dependence of $L(t)$, while $\Delta f \times L_{sys}^2 \gtrsim D$ needs to be satisfied to ensure that the incident energy remains in the sample area at $t = 0$. This is why we set Δf to be 0.05 PHz.

Figure 2 shows the diffusion length $L(t)$ for both polarizations. We can see that the growth of $L^2(t)$ for most frequencies is linear as given by Eq. (4), indicating that such frequencies lie in the effectively delocalized regime. Because most of the incident energy is injected shortly after $t = -t_{inc}/2$, the linear increase begins after $-t_{inc}/2$. The values of the diffusion coefficient D are estimated from the slopes as shown in Figure 3. We find that three dips occur in this frequency range for both polarizations. On the other hand, in the localized regime, we observe suppressed growth of $L^2(t)$ at $f_c = 0.7$ PHz (f_1) and $f_c = 1.2$ PHz (f_2) for TM-mode as shown in Fig. 2 (a). The inset of Figure 2 (a) shows the longtime behavior of f_1 and f_2. From the Eq. (5), ξ is estimated to be about 1.2 μm at f_1 and 1.6 μm at f_2.

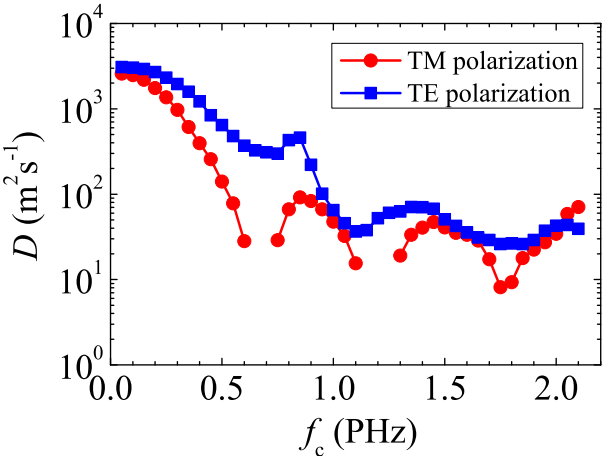

FIG. 3. (Color online) Frequency dependence of the diffusion coefficient D for both polarizations.

If we perform the same calculation for another configuration of columns, the absolute value of D changes a little. However, the overall frequency dependence does not depend on the specific sample configurations, but only on R, Φ, and n. This is not limited to the diffusion length, but is just as valid for the autocorrelation function and the photon lifetime as discussed below.

IV. AUTOCORRELATION FUNCTION

In the case of the diffusion length, the available duration time for the analytical method was limited to about 100 fs for the effectively delocalized regime. In this section, we use the autocorrelation function $C(t)$, in which the available analysis duration time is not limited. The autocorrelation function is defined by

$$C(t) = \frac{1}{t}\int_0^t dt' P(t'), \quad P(t) = \int d\boldsymbol{r}\, \sqrt{u(\boldsymbol{r},0)u(\boldsymbol{r},t)}, \qquad (6)$$

in analogy with a random electron system.[17] The function $P(t)$ denotes the overlap function between the initial spatial distribution of the normalized energy density $u(\boldsymbol{r}, 0)$ at $t = 0$ and

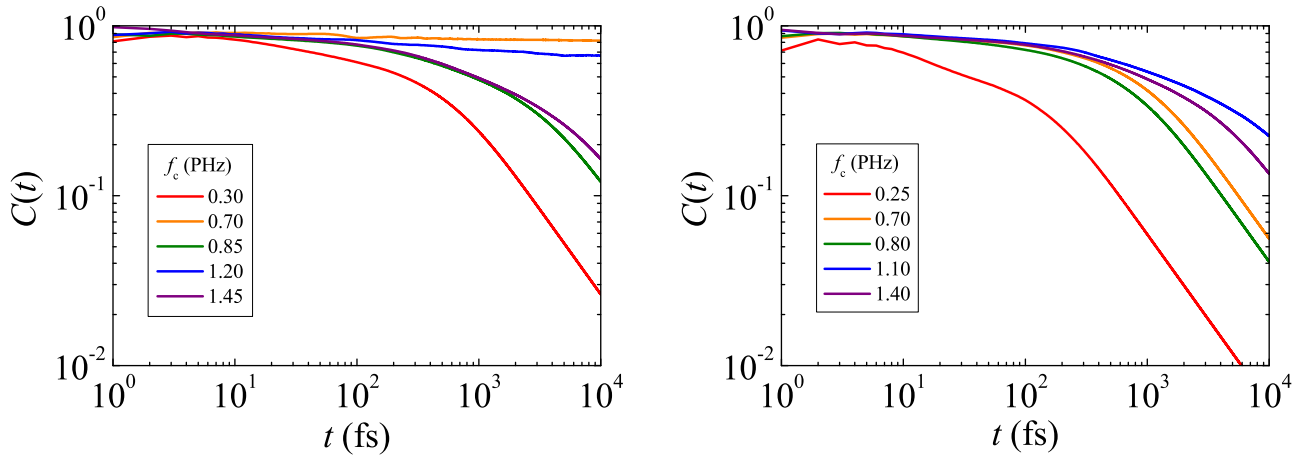

(a) TM polarization

(b) TE polarization

FIG. 4. (Color online) Autocorrelation function $C(t)$ of both polarizations for several f_c.

the distribution of $u(\boldsymbol{r}, t)$ at a given t. Since $P(t)$ fluctuates strongly in time, we use $C(t)$ instead of $P(t)$ to smear out the fluctuation. In the case of the infinite 2D random system, it is expected that both $P(t)$ and $C(t)$ decay in proportion to $t^{-1/2}$ in the delocalized regime, while they remain constant in the limit of large t in the localized regime. On the other hand, in the case of the finite system where the localization length is larger than the system sizes, wave packets eventually touch the boundary of the system and the electromagnetic energy is absorbed. Hence $P(t)$ begins to decay in proportion to $e^{-t/\tau}$, while $C(t)$ is in proportion to t^{-1}.

Figure 4 shows the autocorrelation function $C(t)$ for several f_c. As expected from the behavior of $L(t)$, $C(t)$ around f_1 and f_2 have finite values in the limit of large t in the case of the TM-mode, because the frequency ranges are in the localized regime. On the other hand, for the effectively delocalized regime we can see that at longer times ($t \gtrsim 10^3$ fs) $C(t)$ is in proportion to t^{-1}, respectively, indicating that most of the energy has begun to be absorbed at the boundaries.

In order to investigate the frequency dependence of the autocorrelation function, we have plotted $C(t)$ at $t = 10^4$ fs as a function of f_c, as shown in Figure 5. In both polarizations, we find that there are three peaks corresponding to the three dips in the diffusion coefficient D. We also see that $C(t)$ shows a larger value at each peak and a larger frequency dependence for the TM field than for the TE field.

Although the quantity $C(t)$ is suitable for studying the time dependence of light diffusion for a longer time, we cannot study the frequency dependence in detail because of ambiguity of the frequency of the order of width Δf. In the next section, we show more precisely the frequency dependence of the light localization phenomenon based on a different approach.

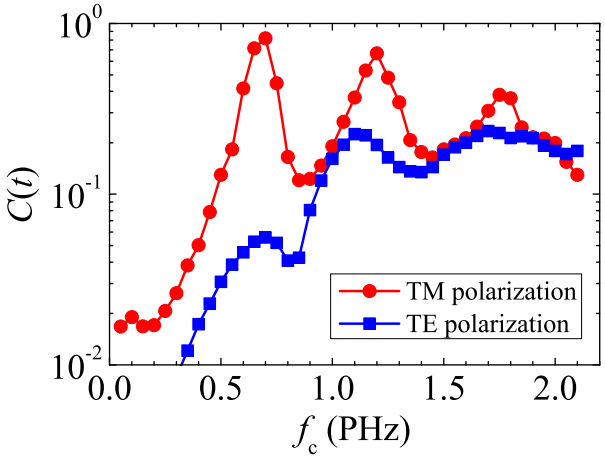

FIG. 5. (Color online) Frequency dependence of the autocorrelation function $C(t)$ of both polarizations at $t = 10^4$ fs.

V. PHOTON LIFETIME

We now adopt another calculation technique to investigate frequency dependence of the light propagation in more detail. Unlike the calculations above, this method gives us information about the light localization over a wide spectrum in a single FDTD simulation. In order to study the parametric dependence of the localization effect, we have simulated temporal propagation and diffusion of a white light source using the FDTD method, and analyzed the simulation results by Fourier transformation. We conducted the simulations on several sample sizes $L_{\mathrm{sys}} = 5$, 10, 15, and 20 μm.

We first irradiated a Gaussian white pulse onto the center of the sample area at $t = 0$. The frequency width of the incident pulse Δf was 10 PHz, resulting in a pulse width of about 0.044 fs. After irradiation, light waves gradually escape through the boundaries because the simulation systems are open. The maximum simulated time t_{max} is 12 ps. In the FDTD simulation, we recorded the temporal evolution of the

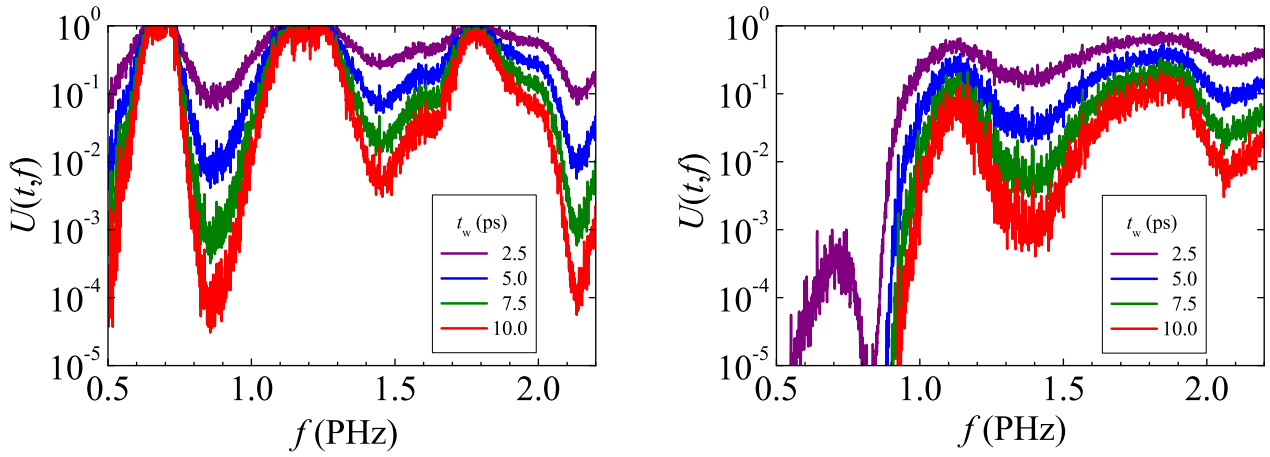

(a) TM polarization

(b) TE polarization

FIG. 6. (Color online) Time dependence of normalized internal energy spectra $U(t, f)$ within the sample system for both polarizations. Each spectrum was obtained by normalizing a spectrum with several time windows by a spectrum with time window [0 ps, 2 ps].

electromagnetic fields by an array of antennas evenly spaced at 100 nm intervals in the systems. We obtained the internal energy spectrum within the systems by averaging all power spectra that were Fourier transformed from signals recorded in a time window $[t_w, t_w + 2\,\text{ps}]$ with each antenna.[19,20] Our analysis looks similar to those presented in Refs. [19,20], but the procedures are different. We performed Fourier transformation on each recorded electric field, and then summed up the obtained frequency spectra. In addition, we used a high dynamic range window function, namely a Nuttall window[21] for the Fourier transformation. This is required since the localization effect has large frequency dependence.

We can investigate time dependence of the internal energy within the systems at several frequencies $U(t, f)$ by changing t_w. Figure 6 shows the spectra collected over several time windows for the system of $L_{sys} = 20$ textmum, each spectrum of which was normalized by a spectrum with time window [0 ps, 2 ps].

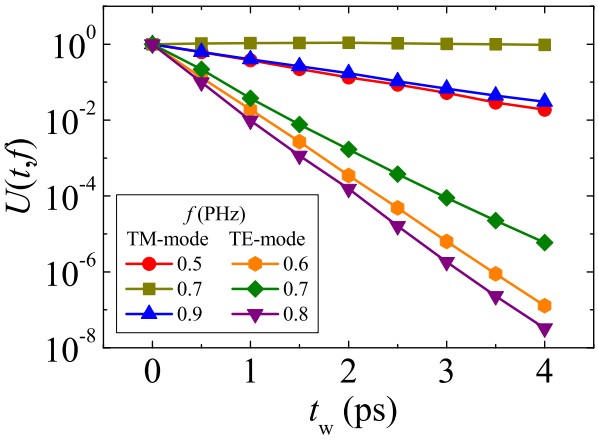

FIG. 7. (Color online) Temporal behavior of normalized internal energy $U(t, f)$ for several time windows. Both cases of polarization are shown.

It is expected that $U(t, f)$ remains constant in the limit of large t in the localized regime, while $U(t, f)$ begins to decay in proportion to $e^{-t/\tau(f)}$ in the effectively delocalized regime, where $\tau(f)$ is the photon lifetime of the system, after wave packets finally reach the boundary. Figure 7 shows temporal changes of $U(t, f)$ for $L_{sys} = 20\,\mu$m. We find that $U(t, f)$ is almost constant at $f = 0.7$ PHz $(= f_1)$, while $U(t, f)$ at the other f decays exponentially. We can estimate $\tau(f)$ from $U(t, f)$ in the delocalized regime. Figure 8 shows the frequency dependence of the lifetime $\tau(f)$ for the TM and TE modes for several system sizes. Note that $U(t, f)$ around f_1 and f_2 remains constant on the time scale of t_{max}, hence $\tau(f)$ cannot be estimated around these frequencies (except for small enough size $L_{sys} = 5\,\mu$m at f_2). The lacks of such points are invisible in the figure.

We obtained precise frequency dependence of the light localization using our method. The fine peaks of the spectra are not noise but due to the localized states and the *almost localized states*[22]. We note that the frequency resolution of the Fourier analysis is not sufficient to separate individual eigenmode. Therefore each fine peak does not correspond to single eigenmode, but originates from the localized states and the almost localized states. These peaks can be random lasing modes if the gain mechanism is introduced in the system. The fine structures depend on the specific column configurations, but the overall frequency dependence is independent of the configurations.

VI. SINGLE PARAMETER SCALING

In this section, we discuss the scaling behavior of light localization with system size L_{sys} and the localization length ξ

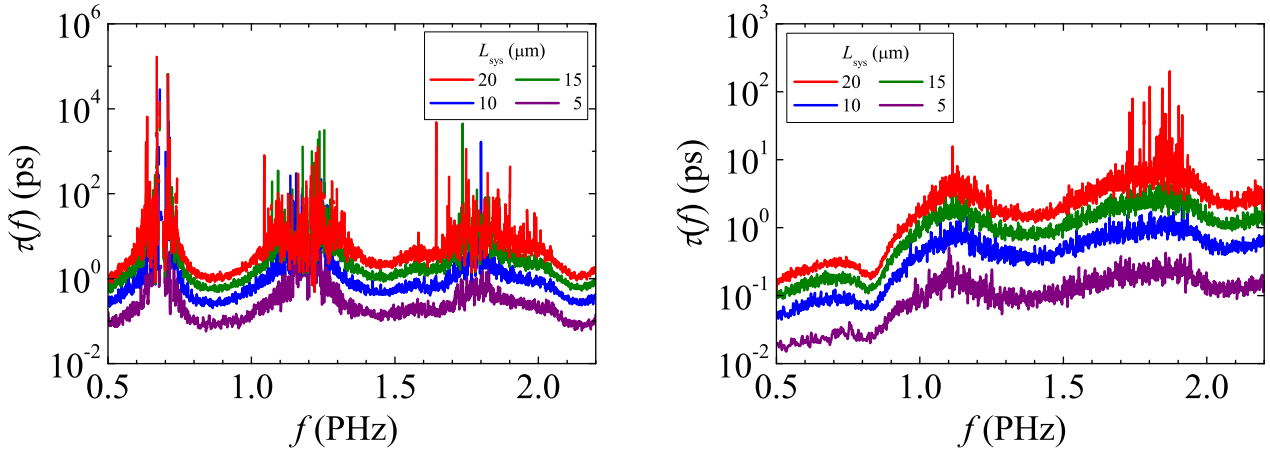

(a) TM polarization

(b) TE polarization

FIG. 8. (Color online) Frequency dependence of the photon lifetime $\tau(f)$ of both polarizations for several system sizes.

in the case of the effectively delocalized regime. We suppose that the photon lifetime τ is expressed as functions of R, Φ, n, $L_{\rm sys}$ and f,

$$T := c\tau/a = F\left(R, \Phi, n, L_{\rm sys}, f\right), \tag{7}$$

where c is the velocity of light in vacuum, and a the average distance of each column. T is interpreted as the average number of times that a light wave encounters the columns before it leaves the system.

In this paper, R, Φ, and n are fixed, while $L_{\rm sys}$ and f are varied, so T varies as

$$T = F\left(L_{\rm sys}, f\right). \tag{8}$$

It also depends on the polarization direction.

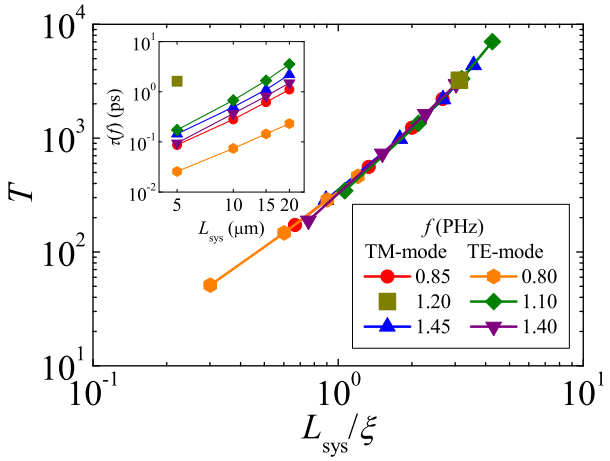

FIG. 9. (Color online) Universal behavior of normalized photon lifetime T and system size dependence of photon lifetime $\tau(f)$ (inset). For the vertical axis T, the average distance is set to be the lattice constant of the triangular photonic crystal with $\Phi = 0.4$.

We assume that the localization length ξ is larger than microscopic length scale such as wave length, a and the mean free path l, so that the function T becomes a single parameter function of a nondimensional quantity $\xi/L_{\rm sys}$,

$$T \approx F\left(\frac{\xi}{L_{\rm sys}}\right). \tag{9}$$

Here the information of f and the polarization is included in ξ, which depends on f and the polarization.

The inset of Figure 9 shows system size dependence of the photon lifetime τ in the effectively delocalized regime, using our data. Each curve is given by averaging the decay rate $1/\tau$ with the range of 0.05 PHz. In this figure, τ at $f = 1.2$ PHz ($= f_2$) can be estimated for $L_{\rm sys} = 5\,\mu$m, while it cannot be estimated for $L_{\rm sys} = 10$, 15, and 20 μm because the states are in the localized regime. In addition, τ at f_1 cannot be estimated for all system sizes. To verify that our results are consistent with Eq. (9), we divide each system size by a certain value, which shifts the curves of the inset horizontally. We find that the shifted curves are on a single curve as shown in Figure 9, confirming the single parameter scaling ansatz.

From the above scaling procedure, we have obtained the frequency dependence of the localization length ξ. Since the scaling procedure determines only the relative values of ξ, we need an independent method to determine ξ at a certain frequency. We therefore used ξ determined from $L(t)$ for TM-mode at f_2 (see the inset of Fig. 2(a)). Figure 10 shows the obtained frequency dependence of the localization length ξ. The behavior of this graph is consistent with the results of $L(f)$, $C(f)$, and $\tau(f)$, that is to say, there are three dips for both polarizations, and two quite small values of $\xi(f)$ appear for TM-mode. Note that the transition region between the effectively delocalized and localized regimes does not locate around $\xi/L_{\rm sys} = 1$. In fact the exponential decay in time is still observed even when $\xi/L_{\rm sys} = 0.2$. We suppose that the crossover of the two regimes exists around $\xi/L_{\rm sys} = 0.2$.

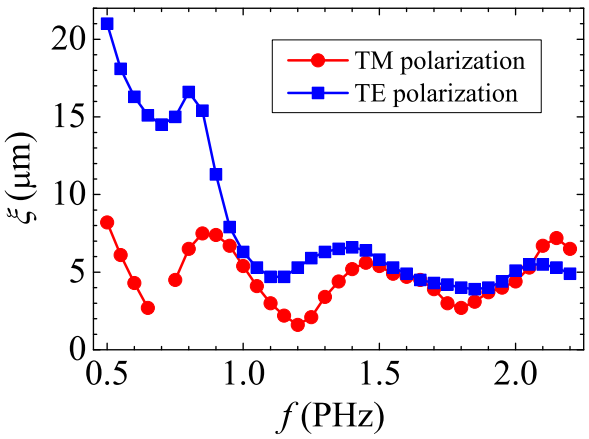

FIG. 10. (Color online) Frequency dependence of the localization length ξ for both polarizations.

VII. ORIGIN OF LIGHT LOCALIZATION

Before concluding, we discuss the physical origin of light localization. We first consider the relationship between Mie resonance of a single column and the light localized regime studied here. Recently, it was reported that in similar systems the frequency dependence of the light localization is independent of the Mie resonance of a single column, but the role of the Mie resonance in light localization is not well understood.[19,20]

Figure 11 shows the frequency dependence of the normalized scattering cross section (SCS) of a single column $\sigma(f)/2R$ for both polarizations, where $\sigma(f)$ is the unnormalized SCS, and is related to the photon mean free path l by $l \sim 1/(N\sigma)$, N is the number density of columns.We find that the peaks of the SCS are not similar to the dips of the localization length spectra. We therefore conclude that the observed phenomena studied here are not simply caused by the Mie resonance effect of a single column[19,20,23,24] but are due to multiple interference effects similar to that observed in photonic crystals[25] as discussed below.

Because the dielectric columns were not in contact with each other, the system was not completely random but the effect of the non-overlapping condition should be taken into account. To examine the degree of randomness, we adopt the index of randomness $D_{\mathrm{R}}(\Phi)$ described by

$$D_{\mathrm{R}} = \frac{(\Delta N)^2}{\bar{N}}, \tag{10}$$

where $\bar{N}$ and $(\Delta N)^2$ respectively denote the average and variance of the number of columns in a wide area. The index $D_{\mathrm{R}}(\Phi)$ approaches unity in the case of complete randomness, while $D_{\mathrm{R}}(\Phi)$ approaches zero in the case of a periodic array of columns. We have calculated $D_{\mathrm{R}}(\Phi)$ for our system with $\Phi = 0.4$ and estimated the value to be 0.09. This small value indicates that the non-overlapping condition is important for our system, which means the system is somewhat periodic. In the systems where columns are positioned periodically, photonic band structures appear and photonic band gaps occur under certain conditions.[26,27] When $D_{\mathrm{R}}(\Phi)$ is quite small, light propagation characteristics similar to those of a periodic system are expected.

In order to consider the physical meaning of frequency dependence of the light localization, we have compared our results with the photonic crystals which consist of a periodic array of the same dielectric circular columns. We have calculated the density of states (DOS) $\rho(f)$ by adopting the same parameters, using the plane wave expansion (PWE) method.[28] Figure 12 shows the DOS for photonic crystals with a triangular lattice and a square lattice. We have used 1261 and 1681 plane waves in total for each wave vector point, respectively, for obtaining these results and have calculated at 33,153 wave vector points. We find that for both polarizations, the frequency ranges in which the DOS is lower are close to the dips shown in Figure 3, and the peaks of the plots in Figures 5 and 8.

In a photonic crystal, the DOS is lower (band gaps are formed in some cases) if Bragg diffraction conditions are satisfied. On the other hand, randomness in the positions of the dielectric columns changes band gaps to pseudogaps, which form the strongly localized regimes, in analogy with amorphous semiconductors.[3] Thus we conclude that the light localization with $\Phi = 0.4$ occurs because of wave interference due to Bragg-like diffraction. This conclusion is not applicable to the whole random systems but limited to the systems with small $D(\Phi)$. When $D(\Phi)$ is quite large, namely in the case of small Φ, it is expected that light propagation characteristics depend mainly on the SCS.

VIII. CONCLUSION

In this paper, we have investigated the frequency dependence of the light localization phenomenon in the 2D random

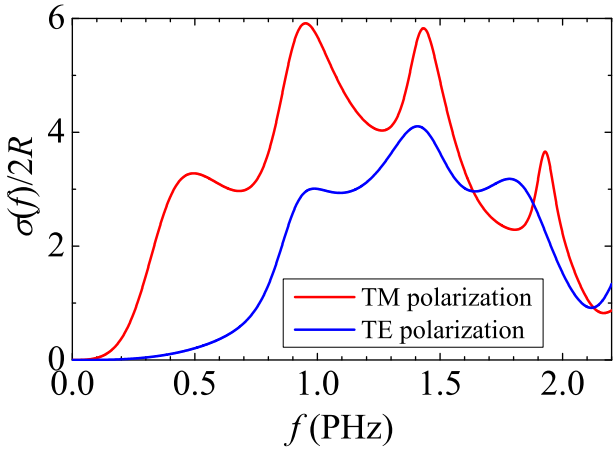

FIG. 11. (Color online) Frequency dependence of the normalized scattering cross section for a single column $\sigma(f)/2R$ for both polarizations. The parameters of the column are the same as before, namely $R = 50$ nm and $n = 2.4$.

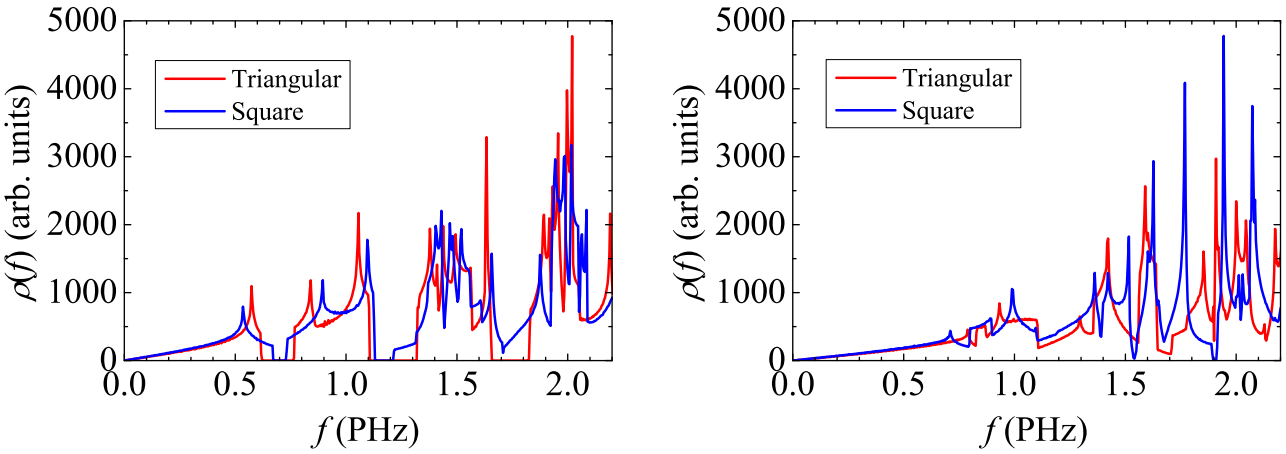

(a) TM polarization

(b) TE polarization

FIG. 12. (Color online) Frequency dependence of the density of states $\rho(f)$ in the case of triangular and square lattice photonic crystals for both polarization.

systems of a dielectric column ensemble, with reference to the parameters of GaN nanocolumn samples. We have calculated the diffusion length, the autocorrelation function of the energy density, and the photon lifetime of the system, using the finite-difference time-domain method. We find that two strongly localized regimes appear for the TM-mode under the adopted parameters. Furthermore, we have succeeded in obtaining the single parameter scaling of the light localization phenomenon and the frequency dependence of the localization length. In addition, we have estimated that the crossover from the effectively delocalized to the localized regime exists when the ratio between the localization length and the system size is nearly 0.2. We conclude that the frequency dependence of the localization phenomenon occurs because of wave interference due to Bragg-like diffraction.

ACKNOWLEDGMENTS

This work was partly supported by Grant-in-Aid for Scientific Researches, #21654042 and #21104518, from the Ministry of Education, Culture, Sports, Science and Technology, Japan.

[1] S. John, Phys. Rev. Lett. **53**, 2169 (1984)
[2] S. John, Phys. Rev. Lett. **58**, 2486 (1987)
[3] S. John, Phys. Today **53**, 32 (1991)
[4] A. R. R. A. F. Ioffe, Prog. Semicond. **4**, 237 (1960)
[5] C. M. Aegerter, M. Storzer, and G. Maret, Europhys. Lett. **75**, 562 (2006)
[6] T. Schwartz, G. Bartal, S. Fishman, and M. Segev, Nature **446**, 52 (2007)
[7] H. Cao, Y. G. Zhao, H. C. Ong, S. T. Ho, J. Y. Dai, J. Y. Wu, and R. P. H. Chang, Appl. Phys. Lett. **73**, 3656 (1998)
[8] H. Cao, Y. G. Zhao, S. T. Ho, E. W. Seelig, Q. H. Wang, and R. P. H. Chang, Phys. Rev. Lett. **82**, 2278 (1999)
[9] H. Cao, J. Xu, D. Z. Zhang, S.-H. Chang, S. T. Ho, E. W. Seelig, X. Liu, and R. P. H. Chang, Phys. Rev. Lett. **84**, 5584 (2000)
[10] S. F. Yu, C. Yuen, S. P. Lau, W. I. Park, and G.-C. Yi, Appl. Phys. Lett. **84**, 3241 (2004)
[11] S. P. Lau, H. Y. Yang, S. F. Yu, H. D. Li, M. Tanemura, T. Okita, H. Hatano, and H. H. Hng, Appl. Phys. Lett. **87**, 013104 (2005)
[12] Y. I. M. Sakai, K. Ema, T. Ohtsuki, H. Sekiguchi, A. Kikuchi, , and K. Kishino, Appl. Phys. Lett. To be published
[13] M. Yoshizawa, A. Kikuchi, M. Mori, N. Fujita, and K. Kishino, Jpn. J. Appl. Phys. **36**, L459 (1997)
[14] A. Taflove and S. C. Hagness, *Computational Electrodynamics: The Finite-Difference Time-Domain Method*, 3rd ed. (Artech House, Norwood, MA, 2005)
[15] E. Abrahams, P. E. Anderson, D. C. Licciardello, and T. V. Ramakrishnan, Phys. Rev. Lett. **42**, 673 (1979)
[16] J. P. Berenger, J. Comput. Phys. **114**, 185 (1995)
[17] T. Kawarabayashi and T. Ohtsuki, Phys. Rev. B **53**, 6975 (1996)
[18] H. D. Raedt, Comp. Phys. Rep. **7**, 1 (1987)
[19] P. Sebbah and C. Vanneste, Phys. Rev. B **66**, 144202 (2002)
[20] C. Vanneste and P. Sebbah, Phys. Rev. E **71**, 026612 (2005)
[21] A. H. Nuttall, IEEE Trans. Acoust. Speech Signal Process. **29**, 84 (1981)
[22] V. M. Apalkov, M. E. Raikh, and B. Shapiro, J. Opt. Soc. Am. B **21**, 132 (2004)
[23] M. M. Sigalas, C. M. Soukoulis, C.-T. Chan, and D. Turner, Phys. Rev. B **53**, 8340 (1996)
[24] A. A. Chabanov and A. Z. Genack, Phys. Rev. Lett **87**, 153901 (2001)
[25] E. Heller, Phys. Rev. Lett. **77**, 4122 (1996)
[26] E. Yablonovitch, Phys. Rev. Lett. **58**, 2059 (1987)
[27] E. Yablonovitch and T. J. Gmitter, Phys. Rev. Lett. **63**, 1950 (1989)

[28] M. Pliha. and A. A. Maradudin, Phys. Rev. B **44**, 8565 (1991)